Scattering of electrons in silicon inversion layers by remote surface roughness

F. Gámiz[a] and J. B. Roldán
Departamento de Electrónica y Tecnología de Computadores, Universidad de Granada, Avd. Fuentenueva s/n, 18071 Granada, Spain

(Received 14 February 2003; accepted 1 April 2003)

A model to study the effect of the roughness at the poly-Si/SiO_2 interface in silicon inversion layers on the electron mobility is obtained. Screening of the resulting perturbation potential by the channel carriers is taken into account, considering Green's functions for metal–oxide–semiconductor geometry, i.e., taking into account the finite thickness of the gate oxide. Mobility of electrons is evaluated at room temperature by the Monte Carlo method, taking into account the simultaneous contribution of phonon scattering, SiO_2/Si interface roughness scattering, Coulomb scattering, and remote surface roughness scattering. The contribution of excited subbands is considered. The resulting remote surface roughness scattering is shown to be strongly dependent on the oxide thickness, and degrades mobility curves at low inversion charge concentrations. The results obtained show that the effect of this scattering mechanism cannot be ignored when the oxide thickness is below 5 nm, (as in actual devices), even when (as is usual) very high doping concentrations are used. © *2003 American Institute of Physics.* [DOI: 10.1063/1.1577227]

I. INTRODUCTION

Scaling complementary metal–oxide–semiconductor (CMOS) devices to smaller dimensions while maintaining good control of the short-channel effects, makes it necessary to reduce the gate oxide thickness in close proportion to the channel length.[1] Thus, for devices with gate lengths below 0.1 μm, gate oxides thinner than 2 nm are needed.[2] The use of such thin oxides leaves inversion layer electrons very near the interface formed by the gate material [metal or polycrystalline silicon (''poly'')] and the oxide, SiO_2. This proximity is sufficient for the transport properties of the electrons in the channel to be modified by the imperfections of this interface:[3] the gate(poly or metal)/oxide interface is not perfectly smooth, and its deviation from an ideal plane (similarly to what happens with the oxide/semiconductor interface) produces a potential modification affecting the electrons in the channel. These potential modifications produce the electron scattering and consequently a degradation in their mobility. Different authors have experimentally shown a mobility degradation as the oxide thickness is reduced.[4–8] Different mechanisms have been proposed as responsible for this mobility decrease: remote Coulomb scattering due to the charges in the depletion layer of the poly-Si,[7,8] long range Coulomb scattering,[9] and even remote surface-roughness scattering.[3]

Li and co-workers developed a theoretical model describing how the electrons in the channel are scattered by the roughness of the gate/oxide interface. They showed that this scattering mechanism is of increasing importance as the gate oxide thickness is decreased to less than 10 nm.[3] In their model Li *et al.* assumed that the metal/oxide interface roughness was due to the fluctuation of the oxide thickness from its average value. They evaluated the change in the potential due to the oxide thickness fluctuation, and calculated the matrix element of the perturbation Hamiltonian in the electric quantum limit (only one subband), assuming the usual variational wavefunction for the ground subband.[10] The electron mobility limited only by this scattering mechanism was then evaluated in the relaxation time approximation. It is shown that this scattering mechanism is more important at low inversion charge concentrations where the contribution of excited subbands to the total transport properties is more important, mainly at room temperature. As a consequence, the contribution of the excited subbands has to be taken into account. Li and Ma obtained their results at very low temperatures, 4.2 K, at which phonon scattering is very weak and can be ignored. The situation at room temperature is completely different since phonon scattering becomes one of the main limitations to electron mobility. Moreover, very high doping concentrations in the MOS channel are required to control short-channel effects.[1] The high concentration of impurities produces an important degree of mobility limitation due to Coulomb scattering, mainly at low inversion charge concentrations. As the inversion charge concentration increases, this scattering mechanism is weakened by the screening of the channel carriers. Therefore, a realistic determination of the effects of the remote surface-roughness scattering at room temperature should take into account the simultaneous participation of the main scattering mechanisms, i.e., phonon scattering, Coulomb scattering and surface roughness scattering (due to the Si/SiO_2 interface). We have developed a model to describe the effect of remote interface roughness scattering on electron mobility (Sec. II). This model can be easily implemented in a Monte Carlo simulator (Sec. III), where, in addition, and simultaneously, the participation of phonon scattering, Coulomb scattering and Si/SiO_2

[a]Author to whom correspondence should be addressed; electronic mail: fgamiz@ugr.es

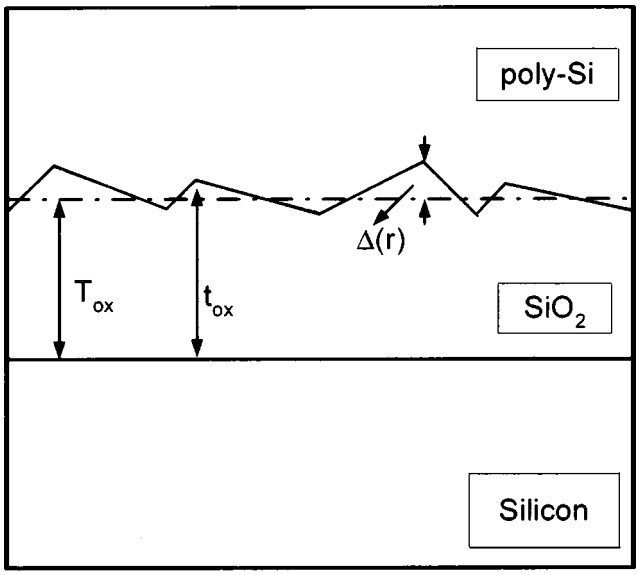

FIG. 1. Schematics of the poysilicon–oxide interface considered in the present work.

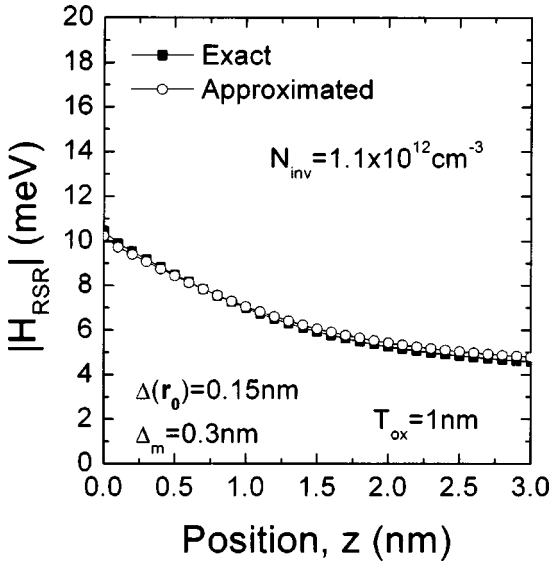

FIG. 2. Perturbation Hamiltonian due to the displacement of $\Delta(\mathbf{r}_0)=0.15$ nm of the poly-SiO_2/Si interface [(bold squares) exact, (open circles) approximated using the mode given in Expression (5)].

interface roughness is considered. Finally, using this Monte Carlo simulator, we calculated electron mobility curves taking into account this new mechanism. Poisson and Schroedinger equations are self-consistently solved in the structure to take into account the quantization of the inversion layer.

II. REMOTE SURFACE ROUGHNESS SCATTERING MODEL

We adopted the idea of Li and co-workers and assumed that the interface roughness is due to the fluctuation of the oxide thickness from its average value, t_{ox}, according to Fig. 1. So, at a given position $\mathbf{r}$ in the plane parallel to the gate, we assumed that the oxide thickness is given by

$$t_{ox}(\mathbf{r})=T_{ox}+\Delta(\mathbf{r}), \tag{1}$$

where T_{ox} is the average oxide thickness and $\Delta(\mathbf{r})$ being the oxide thickness deviations from its average value, which are assumed to be correlated. This correlation is measured by the autocovariance function, which is assumed to follow an exponential law,[11] assuming a behavior similar to that of the oxide/semiconductor interface

$$\langle\Delta(\mathbf{r})\Delta(\mathbf{r}'-\mathbf{r})\rangle=\Delta_m e^{-\sqrt{2}r/L}, \tag{2}$$

where Δ_m is the rms value of the oxide thickness fluctuations and L is the autocovariance length.

At this point $\mathbf{r}$, the potential well in the direction perpendicular to the interface is slightly different from the one corresponding to the ideal case (oxide thickness equal to the average T_{ox}). Let $V^0_{T_{ox}}(z)$ be the potential well in the direction perpendicular to the interface in the ideal case, that is to say, for an oxide thickness equal to the average T_{ox}, and $V_{t_{ox}}(\mathbf{r},z)$ the potential well in the direction perpendicular to the interface, at a point $\mathbf{r}$ in the plane parallel to the gate where the oxide thickness is given by Eq. (1). The remote surface roughness perturbation Hamiltonian is then given by

$$H_{RSR}(\mathbf{r},z)=-e[V_{t_{ox}}(\mathbf{r},z)-V^0_{T_{ox}}(z)]. \tag{3}$$

We have assumed that the two interfaces, poly-Si/SiO_2 and SiO_2/Si are not correlated at all, and that the superposition principle is valid, i.e., we consider the remote surface roughness scattering and the usual surface roughness scattering (due to the SiO_2/Si interface) as two different and independent scattering mechanisms. Thus, when we evaluate the surface roughness scattering rate (due to the fluctuations of the SiO_2/Si interface from an ideal plane) we assume that the oxide thickness is uniform for the whole device. On the other hand, for the evaluation of the remote surface roughness scattering (due to the fluctuations of the poly-Si/SiO_2 interface from an ideal plane) we assume that the SiO_2/Si is an ideal plane, as shown in Fig. 1.

To obtain an expression for the remote surface roughness scattering rate Eq. (3) must be linearized. To do this we assume that the perturbed potential well $V_{t_{ox}}(\mathbf{r},z)$ can be expressed as

$$V_{t_{ox}}(\mathbf{r},z)=V^0_{T_{ox}}(z)+\frac{V_{T_{ox}}+\Delta_m(z)-V^0_{T_{ox}}(z)}{\Delta_m}\Delta(\mathbf{r}), \tag{4}$$

where $V_{T_{ox}}+\Delta_m(z)$ is the potential well in the direction perpendicular to the interface for an oxide thickness equal to $T_{ox}+\Delta_m$. With this assumption, the perturbation Hamiltonian is expressed as

$$H_{RSR}(\mathbf{r},z)=-\frac{e\Delta V_m(z)}{\Delta_m}\Delta(\mathbf{r}), \tag{5}$$

where

$$\Delta V_m(z)=V_{T_{ox}}+\Delta_m(z)-V^0_{T_{ox}}(z). \tag{6}$$

The goodness of this approximation must now be tested. Figure 2 compares the perturbation Hamiltonian given by Expression (5) (open circles) with the exact perturbation Hamiltonian given by Expression (3) (closed squares) for a point $\mathbf{r}_0$ in the plane parallel to the interface where the oxide thickness is $t_{ox}=T_{ox}+\Delta(\mathbf{r}_0)$, with $T_{ox}=1$ nm, and $\Delta(\mathbf{r}_0)=0.15$ nm. The rms value of the oxide thickness fluctuations, Δ_m, is assumed to be 0.3 nm. As observed, the two curves almost coincide, thus proving that the proposed model accurately reproduces the exact perturbation Hamiltonian.

Using this approximation for the perturbation Hamiltonian, the matrix element for remote surface roughness scattering in the Born approximation is then given as

$$|M_{\mu\nu}(\mathbf{q})|^2=|\langle\nu,\mathbf{k}|H_{\mathrm{RSR}}|\mu,\mathbf{k}'\rangle|^2 = e^2\left|\int \psi_\nu(z)\frac{\Delta V_m(z)}{\Delta_m}\psi_\mu(z)dz\right|^2|\Delta(\mathbf{q})|^2, \tag{7}$$

where $\mathbf{k}'$ is the electron wave vector before the scattering, $\mathbf{k}$ the electron wavevector after the scattering, $\mathbf{q}=\mathbf{k}-\mathbf{k}'$, e is the electron charge, $\psi_\mu(z)$ the envelope function in the μth subband, and $\Delta(\mathbf{q})$ is the Fourier transform of $\Delta(\mathbf{r})$. Therefore, to evaluate this matrix element, we have to previously evaluate $\Delta V_m(z)$ according to Eq. (6). Using the exponential model given by Eq. (2) for $\Delta(\mathbf{r})$, $|\Delta(\mathbf{q})|^2$ is given by[12]

$$|\Delta(\mathbf{q})|^2=\frac{\pi\Delta_m^2L^2}{\left(1+\frac{q^2L^2}{2}\right)^{3/2}}. \tag{8}$$

The surface-roughness scattering rate for an electron with wave vector $\mathbf{k}$ in the μ subband and final state in the ν subband is given by

$$\frac{1}{\tau_{\mathrm{RSR},\mu\nu}(\mathbf{k})}=\frac{m_d e^2\Delta_m^2L^2}{2\hbar^3}\times\int_0^{2\pi}\frac{|\Gamma_{\mu\nu}(\mathbf{q})|^2}{\left(1+\frac{L^2q^2}{2}\right)^{3/2}}d\theta \tag{9}$$

with

$$\Gamma_{\mu\nu}(\mathbf{q})=\int \psi_\nu(z)\frac{\Delta V_m(z)}{\Delta_m}\psi_\mu(z)dz \tag{10}$$

and

$$q^2=2k^2(1-\cos\theta). \tag{11}$$

The surface roughness scattering potential is affected by the screening of the mobile electrons in the inversion layer.[13,14] To include the effect of the screening we adopted the procedure developed by Fischetti and Laux in Ref. 14. Thus, the intrasubband matrix elements of the screened scattering potential are given by

$$\Gamma_{\mu\mu}^{\mathrm{screened}}(\mathbf{q})=\Gamma_{\mu\mu}(\mathbf{q}) -2\epsilon_{\mathrm{Si}}\sum_\lambda q_{s,\lambda}(q)\mathsf{F}_{\mu\mu,\lambda\lambda}(q)\Gamma_{\lambda\lambda}^{\mathrm{screened}}(\mathbf{q}), \tag{12}$$

where ϵ_{Si} is the dielectric constant of the silicon and $q_{s,\mu}(\mathbf{q})$ is the screening parameter given by

$$q_{s,\mu}(q)=\frac{e^2}{2\epsilon_{\mathrm{Si}}}\frac{\partial n_\mu}{\partial E_F}g_1(q\lambda_\mu), \tag{13}$$

where n_μ is the population of the μth subband, E_F the Fermi level, λ_μ the thermal wavelength of electrons in the subband μ, and the function $g1(x)$ is defined in Ref. 14. $\mathsf{F}_{\mu\mu,\lambda\lambda}(q)$ is given by

$$\mathsf{F}_{\mu\mu,\lambda\lambda}(q)=\int dz\int dz_1\psi_\mu(z)\psi_\mu(z) \times G_q(z,z_1)\psi_\lambda(z_1)\psi_\lambda(z_1),$$

where $G_q(z,z_1)$ is the Green's functions for a MOS structure, that is to say, taking into account the finite oxide thickness T_{ox}

$$G_q(z,z_1)=\frac{1}{2\epsilon_{\mathrm{poly}}q}e^{-q|z-z_1|} +\left(\frac{A}{2q}-\frac{1}{2\epsilon_{\mathrm{poly}}q}\right)e^{-q(|z|+|z_1|)} +\frac{A}{2q}\frac{\epsilon_{ox}-\epsilon_{sc}}{\epsilon_{ox}+\epsilon_{sc}}e^{-q(|T_{ox}-z_1|+T_{ox}+|z|)} \quad \text{for } z<0, \tag{14}$$

$$G_q(z,z_1)=\frac{1}{2\epsilon_{ox}q}e^{-q|z-z_1|}+\frac{A}{4q}\left(1-\frac{\epsilon_{\mathrm{poly}}}{\epsilon_{ox}}\right)e^{-q(|z|+|z_1|)} +\frac{B}{4q}\left(1-\frac{\epsilon_{sc}}{\epsilon_{ox}}\right)e^{-q(|T_{ox}-z|+|T_{ox}-z_1|)} +\frac{C}{4q}e^{-Q[(T_{ox}-z)+T_{ox}+|z_1|]} +\frac{C}{4q}e^{-q(z+T_{ox}+|T_{ox}-z_1|)} \quad \text{for } 0<z<T_{ox}, \tag{15}$$

$$G_q(z,z_1)=\frac{1}{2\epsilon_{sc}q}e^{-q|z-z_1|} +\left(\frac{B}{2q}-\frac{1}{2\epsilon_{sc}q}\right)e^{-q(|z-T_{ox}|+|z_1-T_{ox}|)} +\frac{B}{2q}\frac{\epsilon_{ox}-\epsilon_{\mathrm{poly}}}{\epsilon_{ox}+\epsilon_{\mathrm{poly}}}e^{-q(z+|z_1|)} \quad \text{for } z>T_{ox}, \tag{16}$$

where the coefficients A, B, and C are given by

$$A=\frac{2(\epsilon_{ox}+\epsilon_{sc})}{(\epsilon_{ox}+\epsilon_{poly})(\epsilon_{ox}+\epsilon_{sc})-e^{-2qT_{ox}}(\epsilon_{ox}-\epsilon_{poly})(\epsilon_{ox}-\epsilon_{sc})}, \tag{17}$$

$$B=\frac{2(\epsilon_{ox}+\epsilon_{poly})}{(\epsilon_{ox}+\epsilon_{poly})(\epsilon_{ox}+\epsilon_{sc})-e^{-2qT_{ox}}(\epsilon_{ox}-\epsilon_{poly})(\epsilon_{ox}-\epsilon_{sc})}, \tag{18}$$

$$C=\frac{2(\epsilon_{ox}-\epsilon_{poly})(\epsilon_{ox}-\epsilon_{sc})}{\epsilon_{ox}[(\epsilon_{ox}+\epsilon_{poly})(\epsilon_{ox}+\epsilon_{sc})-e^{-2qT_{ox}}(\epsilon_{ox}-\epsilon_{poly})(\epsilon_{ox}-\epsilon_{sc})]}. \tag{19}$$

These expressions coincide, although using a unified form, with the ones calculated by Fischetti and Laux in Appendix B of Ref. 9.

Similarly, the intersubband scattering transition is given by[14]

$$\Gamma_{\mu\nu}^{\text{screened}}(\mathbf{q})=\Gamma_{\mu\nu}(\mathbf{q})-2\epsilon_{Si}\sum_{\lambda} q_{s,\lambda}(q) \times F_{\mu\nu,\lambda\lambda}(q)\Gamma_{\lambda\lambda}^{\text{screened}}(\mathbf{q}). \tag{20}$$

Finally the surface-roughness scattering rate for an electron with wave vector $\mathbf{k}$ in the μ subband and final state in the ν subband is given by

$$\frac{1}{\tau_{RSR,\mu\nu}(\mathbf{k})}=\frac{m_d e^2\Delta_m^2 L^2}{2\hbar^3}\times\int_0^{2\pi}\frac{|\Gamma_{\mu\nu}^{\text{screened}}(\mathbf{q})|^2}{\left(1+\frac{L^2q^2}{2}\right)^{3/2}}d\theta. \tag{21}$$

III. MONTE CARLO CALCULATION OF ELECTRON MOBILITY

After having evaluated the scattering matrix elements due to the roughness of the poly-Si/SiO_2 interface, this scattering mechanism was added to a one-electron Monte Carlo simulator[15,16] previously developed, in which, in addition, phonon scattering, surface-roughness scattering (due to the SiO_2/Si interface fluctuations) and Coulomb scattering (due to doping impurities and interface-trapped charges) are taken into account. The Monte Carlo method is held to provide a more rigorous description of device physics than models based on the solution of fundamental balance equations.

Electron quantization in the silicon inversion layer has been taken into account, self-consistently solving the Poisson and Schroedinger equations (a detailed description of this simulation can be found elsewhere).[15–17] In this study, a nonparabolic six equivalent ellipsoidal Δ valleys model was assumed for the silicon conduction band, taking $\alpha=0.5\ \text{eV}^{-1}$, with α being the parameter of nonparabolicity. This limited our study to low-electron energies (below 0.5 eV). We considered the poly-Si/SiO_2 and the SiO_2/Si interfaces to be parallel to a [100] plane. In these conditions, the quantum size effects meant that the degeneracy of the six equivalent minima of the silicon conduction band breaks and the electrons were distributed into two sets of subbands:[13] one set resulted from the two equivalent valleys showing the longitudinal mass in the direction perpendicular to the interface ($\mathbf{E}_1,\mathbf{E}_2,\ldots$). and the other one from the four equivalent valleys showing the transverse effective mass in the same direction ($\mathbf{E}_1',\mathbf{E}_2',\ldots$). The electron effective masses were assumed to be those obtained for the silicon bulk:[13,18] $m_t=0.19m_0$, $m_l=0.98m_0$, with m_0 being the free-electron mass.

For the phonon scattering, we considered acoustic deformation potential scattering and intervalley phonon events. The coupling constants for the intervalley phonons and the acoustic deformation potential were the same as in bulk silicon inversion layers.[18,14] The phonon-scattering rates for inversion layers were deduced by using Price's formulation.[19] Here again, the use of bulk phonons is questionable, as the presence of Si–SiO_2 interfaces undoubtedly alters the dispersion of the phonons, their nature, and their coupling to the electrons. Previous studies[20] taking these effects into account in very idealized conditions showed that phonon-limited mobility is reduced by 20% or less[14] due to the presence of the Si/SiO_2 interfaces. Nevertheless, if such idealized conditions are relaxed, an even lower reduction is expected. For these reasons and due to the difficulty of dealing with the effects of the interfaces on the phonon-scattering rate,[14,20] we ignored such effects, and assumed that bulk phonons are not influenced by the layered structure. For surface roughness scattering, the Ando model was taken into account,[13] screening the potential by means of the method developed in Refs. 14 and 21. Finally, Coulomb scattering was included using the model developed in Refs. 15 and 22. In our simulation, the electron energy was limited to 0.5 eV, since for higher electron energies the results obtained by the simulation are not likely to be very accurate, as a detailed bandstructure was not used. Accordingly, as the silicon band gap was set to 1.12 eV at room temperature (thereby setting the energy threshold for the impact ionization process), impact ionization was not included.

IV. RESULTS AND DISCUSSION

In the present work we attempt to show the effect of remote surface roughness scattering on electron mobility in silicon inversion layers with ultrathin oxide. To do so, we calculated electron mobility curves for different silicon dioxide layer thicknesses and different interface roughness parameters at room temperature, using the Monte Carlo simulator described above. In these calculations, we simultaneously took into account the contribution of the other scattering mechanisms which are important in these devices, in order to determine whether the real effect of this new scattering mechanism is masked, in practice, by the other scattering mechanisms. This is the reason why the first thing we did was to calculate electron mobility curves taking

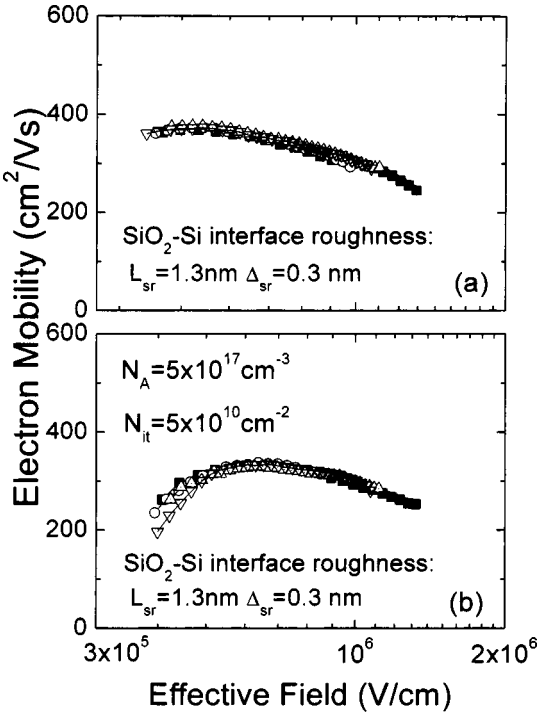

FIG. 3. Electron mobility curves vs the transverse effective field for different values of oxide thickness taking into account: (a) phonon scattering and surface roughness scattering and (b) Coulomb scattering, phonon scattering and surface roughness scattering ($N_A=5\times10^{17}$ cm^{-3}). No remote surface roughness scattering is considered. [(■): $T_{ox}=1$ nm; (○): $T_{ox}=2$ nm; (△): $T_{ox}=5$ nm; (▽): $T_{ox}=10$ nm]

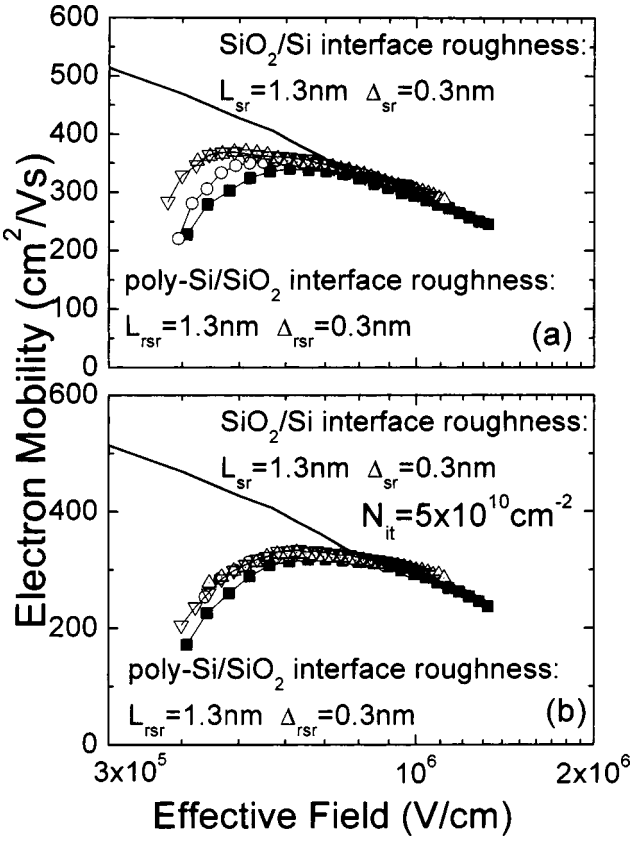

FIG. 4. Electron mobility curves vs the transverse effective field for different values of oxide thickness taking into account: (a) remote surface roughness scattering, phonon scattering, and surface roughness scattering and (b) remote surface roughness scattering, Coulomb scattering, phonon scattering, and surface roughness scattering ($N_A=5\times10^{17}$ cm^{-3}). The parameters for remote surface roughness scattering are given by: $\Delta_{rsr}=0.3$ nm, $L_{rsr}=1.3$ nm. [(■) $T_{ox}=1$ nm; (○) $T_{ox}=2$ nm; (△) $T_{ox}=5$ nm; (▽) $T_{ox}=10$ nm]. For the sake of comparison, universal mobility curve is shown in solid line.

into account the usual scattering mechanisms (phonon, Coulomb, and surface roughness scattering) in a standard ultrathin oxide MOS field effect transistor, ignoring the effect of the remote surface roughness scattering. We considered a MOS structure with the following technological parameters: substrate doping concentration $N_A=5\times10^{17}$ cm^{-3}, interface trap concentration $N_{it}=5\times10^{10}$ cm^{-2}, SiO_2-Si interface roughness parameters: $L_{sr}=1.3$ nm, $\Delta_{sr}=0.3$ nm, and different oxide thicknesses ranging from $T_{ox}=1$ nm to $T_{ox}=10$ nm. A N^+-polysilicon gate with an impurity concentration of $N_D=1\times10^{20}$ cm^{-3} was assumed.

Figure 3 shows mobility curves versus the transverse electric field for different values of the oxide thickness. In Fig. 3(a) only phonon scattering and surface roughness scattering were taken into account, while in Fig. 3(b) the effect of Coulomb scattering due to substrate doping impurities and interface charges is added. Figure 3(a) shows there is no dependence of mobility on the oxide thickness when only phonon and surface roughness are taken into account, but when the effect of the Coulomb scattering is included [Fig. 3(b)] a slight dependence on the oxide thickness appears. In theory, and for a given value of the transverse effective field (or inversion charge concentration) the only dependence of these scattering mechanisms on the oxide thickness arises from the screening of the scattering potentials [Expressions (14)–(19)].

Using for the poly-Si/SiO_2 interface remote surface roughness (RSR) the same parameters used for the SiO_2-Si, our Monte Carlo simulator incorporates the effect of the RSR scattering. Figure 4 shows the same mobility curves as in Fig. 3, but also incorporates the effect of RSR scattering with the model developed in Sec. II. Figure 4(a) shows the electron mobility when Coulomb scattering is ignored. The effect of RSR scattering is to make electron mobility strongly decrease at low inversion charge concentrations. To understand this behavior, we compared the perturbation Hamiltonian for two values of the inversion charge concentration in a MOS structure with an average oxide thickness $T_{ox}=1$ nm, at a point $\mathbf{r}_0$ of the plane parallel to the interface where the fluctuation of oxide thickness is $\Delta(\mathbf{r}_0)=0.15$ nm, and the rms value of the oxide thickness fluctuations, Δ_m, was assumed to be 0.3 nm. Figure 5 shows on the left axis the perturbation Hamiltonian [Expression (3)] for both N_{inv} values. As N_{inv} increases, the difference in the potential well is more acute at the interface, but quickly vanishes as we move to the bulk silicon. On the contrary, for low N_{inv} values, H_{RSR} is weaker at the interface but decreases more slowly toward the silicon bulk. Figure 5 also shows on the right axis the wave functions of the electrons in the ground subband in both cases. As expected, the higher the N_{inv}, the greater the confinement of the electrons towards the interface, and therefore, the less the penetration of the wave functions inside the silicon bulk. The

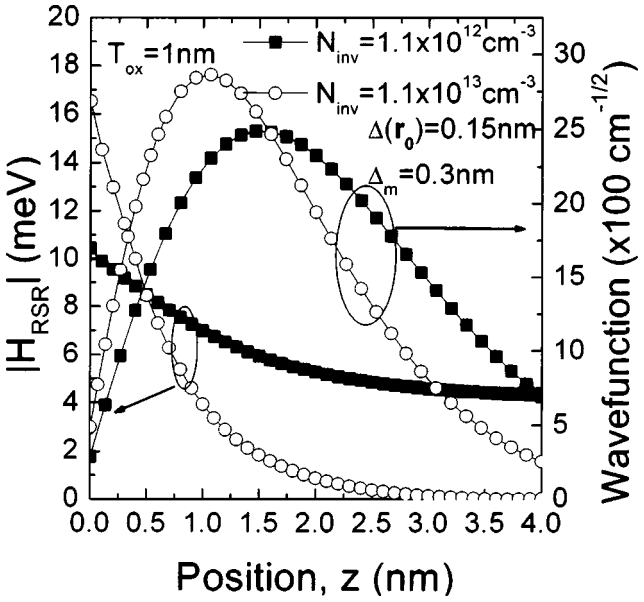

FIG. 5. Perturbation Hamiltonian due to deviation of the poly/SiO_2 from an ideal plane for two different values of the inversion charge concentrations. Also shown, the wave functions for the ground subband at the same inversion charge concentrations.

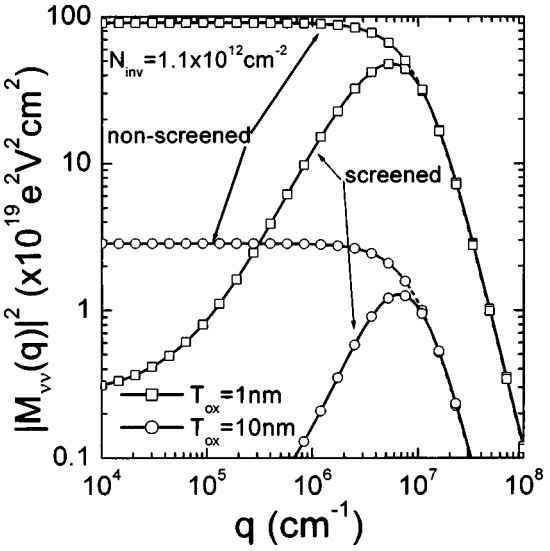

FIG. 7. Matrix element for the ground subband for remote surface roughness scattering for different values of the oxide thickness. The effect of screening is also shown. Inversion charge concentration has been assumed to be $N_{\mathrm{inv}}=1.1\times10^{12}$ cm^{-2}.

scattering matrix element [Expression (7)] receives both the contribution of the perturbation Hamiltonian and of the wave functions. Figure 5 shows how the decrease in the perturbation Hamiltonian is produced faster than the movement of the wave functions towards the SiO_2-Si interface. As a consequence, the net effect is a decrease in the remote surface roughness matrix element as the inversion charge concentration increases, as shown in Fig. 6 (dashed lines). In addition, as the inversion charge increases, the potential scattering is more strongly screened by the mobile carriers. This can be observed in Fig. 6 (solid lines), where the matrix elements for intrasubband transitions in the ground subband is shown for both N_{inv} values: screening reduces both matrix elements, although its effect is more important for high values of the inversion charge concentration. For the sake of comparison, Fig. 6 also shows the matrix element corresponding to an intermediate inversion charge concentration ($N_{\mathrm{inv}}=5.2\times10^{12}$ cm^{-3} in triangles). Figure 4(a) shows there is a strong dependence of the remote surface roughness scattering with the oxide thickness, i.e., mobility curves for $T_{\mathrm{ox}}=10$ nm and $T_{\mathrm{ox}}=5$ nm almost coincide, but for oxide thicknesses lower than 5 nm a strong degradation appears in the mobility, mainly at low inversion charge concentrations. With greater oxide thicknesses, fluctuations in the thickness are, as expected, much less important: Fig. 7 shows the matrix element for intrasubband transitions in the ground subband at low inversion charge concentrations ($N_{\mathrm{inv}}=1.1\times10^{12}$ cm^{-2}) for two values of T_{ox}: $T_{\mathrm{ox}}=1$ nm (squares) and $T_{\mathrm{ox}}=10$ nm (circles). The matrix elements for the thicker oxides are almost 2 orders of magnitude lower than those corresponding to thinner oxides.

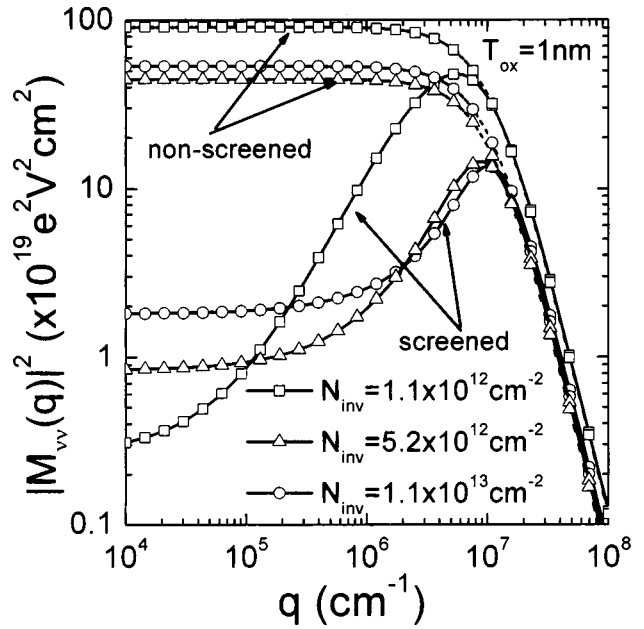

FIG. 6. Matrix element for the ground subband for remote surface roughness scattering for different values of the inversion charge concentration. The effect of screening is also shown. Oxide thickness has been assumed to be $T_{\mathrm{ox}}=1$ nm.

Figure 4(a) shows how the mobility limited by the remote surface roughness scattering behaves qualitatively in a similar way to that due to Coulomb scattering, that is to say, it is very important for low inversion charge concentrations, and starts to increase as the inversion charge concentration increases. Figure 4(a) shows that remote surface roughness scattering is an important scattering mechanism that should be taken into account when oxide thickness is thin enough. However, when Coulomb scattering is also considered, the effects of this new scattering source are partially masked by the contribution of Coulomb scattering. This is illustrated in Fig. 4(b), which shows the same mobility curves as in Fig. 4(a) but incorporates the contribution of Coulomb scattering, due to the ionized doping impurities ($N_A=5\times10^{17}$ cm^{-3})

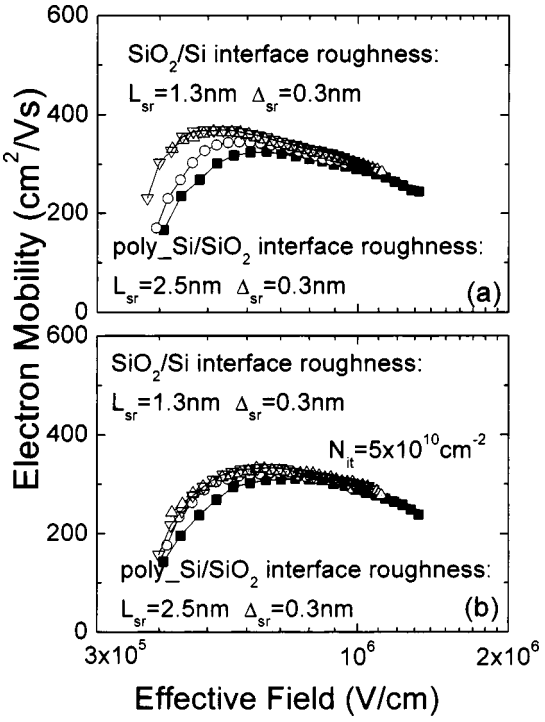

FIG. 8. Electron mobility curves vs the transverse effective field for different values of oxide thickness taking into account: (a) remote surface roughness scattering, phonon scattering, and surface roughness scattering and (b) remote surface roughness scattering, Coulomb scattering, phonon scattering, and surface roughness scattering ($N_A=5\times10^{17}$ cm^{-3}). The parameters for remote surface roughness scattering are given by $\Delta_{rsr}=0.3$ nm, $L_{rsr}=2.5$ nm. [(■) $T_{ox}=1$ nm; (○) $T_{ox}=2$ nm; (△) $T_{ox}=5$ nm; (▽) $T_{ox}=10$ nm]

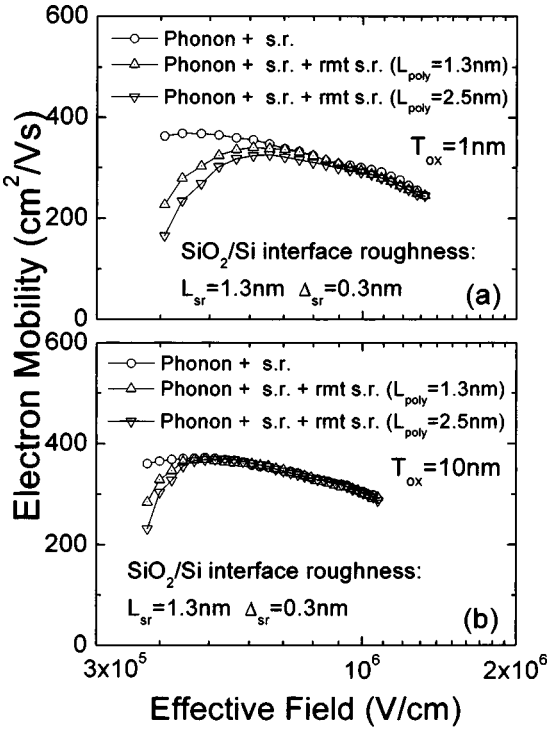

FIG. 9. Electron mobility curves for different values of the oxide thickness: (a) $T_{ox}=1$ nm, (b) $T_{ox}=10$ nm: (circles) only phonon and surface roughness scattering are taken into account; (up triangles) remote surface roughness scattering with an autocovariance length, $L_{rsr}=1.3$ nm is added to phonon scattering and surface roughness scattering; (down triangles) remote surface roughness scattering with an autocovariance length, $L_{rsr}=2.5$ nm is added to phonon scattering and surface roughness scattering.

and to the presence at the Si–SiO_2 interface of a interface trapped charge concentration of $N_{it}=5\times10^{10}$ cm^{-2}. The dependence of the mobility on the oxide thickness is much less acute in this second case, which means a lesser contribution of remote surface roughness scattering to the total mobility. Figure 8 shows the same mobility curves as in Fig. 4 but with a higher correlation length for the roughness of the poly-Si/SiO_2 interface, $L_{rsr}=2.5$ nm. According to Expression (8), a higher L implies a higher scattering rate and therefore a lower mobility curve. These effects are more evident in Fig. 9, which shows the different contributions to the electron mobility of two values of the oxide thickness: $T_{ox}=1$ nm [Fig. 9(a)] and $T_{ox}=10$ nm [Fig. 9(b)] ignoring the effect of Coulomb scattering while in Fig. 10 the Coulomb scattering due to the bulk ionized impurities and to the interface trapped charges are taken into account. These figures show that the effect of remote surface roughness scattering is very weak for oxide thicknesses greater than $T_{ox}=10$ nm, where its effect can be ignored. However, for thinner oxide layers, $T_{ox}<2$ nm, remote surface roughness is as important as Coulomb scattering, even when, as happens here, the doping concentration, and therefore the Coulomb scattering, is very strong. Therefore, in conclusion, the effect of remote surface roughness scattering has to be taken into account in the calculation of electron mobility curves in ultrathin oxide inversion layers.

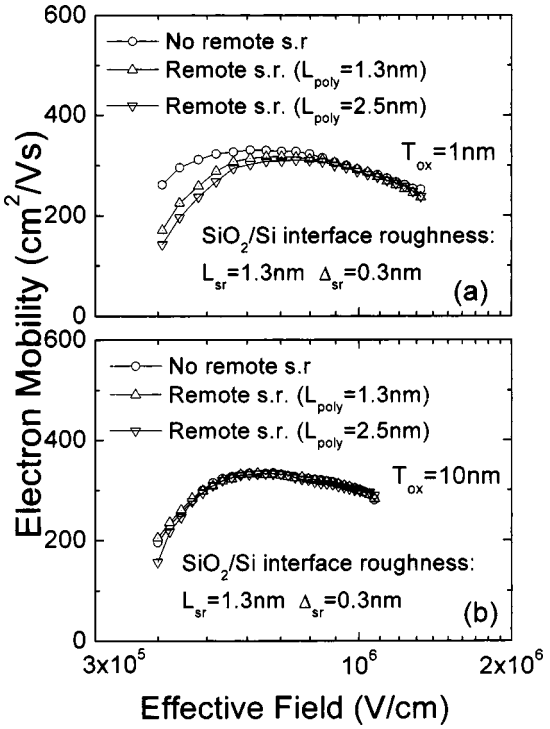

FIG. 10. The same as Fig. 9, but taking into account the effects of Coulomb scattering.

Finally, we would like to bring the reader's attention to the fact that until now, and in the development of the model described here, it has been assumed that the two interfaces, (poly-Si/SiO_2, and SiO_2/Si interfaces) are not correlated at all. In consequence, two independent and different scattering mechanisms exist [triangles in Fig. 10(a)]. This is true for high oxide thickness values. However, as the oxide thickness is reduced, a certain degree of correlation between the two interfaces is expected. The limit situation occurs when the two interfaces are conformal. This implies a constant oxide thickness and therefore a null remote surface roughness scattering; in such a case, only the surface roughness scattering due to the fluctuations of the SiO_2/Si interface from an ideal plane would exist [circles in Fig. 10(b)]. The actual situation is a case in between the two extremes, and depends on the degree of correlation between the two interfaces. Thus, the actual mobility curve lies between the two mobility curves shown in Fig. 10(a). The proximity of the actual curve to one or the other curve will depend on the degree of correlation between the two interfaces, and, probably, on the oxide thickness.

V. CONCLUSIONS

We have obtained a model to study the effect of the roughness at the poly-Si/SiO_2 interface in silicon inversion layers on electron mobility (remote surface roughness scattering). Screening of the resulting perturbation potential by the channel carriers is taken into account, considering Green's functions for MOS geometry, i.e., taking into account the finite thickness of the gate oxide. Electron mobility is evaluated at room temperature by the Monte Carlo method by taking into account the simultaneous contribution of phonon scattering, SiO_2/Si interface roughness scattering, Coulomb scattering, and remote surface roughness scattering. The contribution of excited subbands is also taken into account. We observed that remote surface roughness limited mobility behaves in a similar way to Coulomb scattering as the inversion charge increases, that is, it increases as the inversion charge increases. This is explained in terms of the perturbation Hamiltonian and the screening effect. The resulting remote interface roughness scattering is strongly dependent on the oxide thickness, and for currently available devices, the effect of this scattering mechanism cannot be ignored, even when, as usual, very high doping concentrations are used.

ACKNOWLEDGMENT

This work has been carried out within the framework of Research Project No. TIC2001-3243 supported by the Spanish Government.

[1] SIA Roadmap, 1999
[2] H. S. Momose *et al.* Tech. Dig. - Int. Electron Devices Meet. **1996**, 109.
[3] J. Li and P. Ma, J. Appl. Phys. **62**, 4212 (1987).
[4] A. Chin, W. J. Chen, T. Chang, R. H. Kao, B. C. Lin, C. Tsai, and J. C. M-Huang, IEEE Electron Device Lett. **18**, 417 (1997).
[5] M. S. Krishnan, L. Chang, T. King, J. Bokor, and C. Hu, Tech. Dig. - Int. Electron Devices Meet. **1999**, 241.
[6] M. Alam, B. Weir, and P. Silverman, Extend. Abst. International Workshop on Gate Insulators, 2001, p. 30.
[7] S. Takagi and M. Takayanagi, Jpn. J. Appl. Phys., Part 1 **41**, 2348 (2002).
[8] S. Saito, K. Torii, M. Hiratani, and T. Onai, Appl. Phys. Lett. **81**, 2391 (2002).
[9] M. V. Fischetti and S. E. Laux, J. Appl. Phys. **89**, 1205 (2001).
[10] F. Stern and W. E. Howard, Phys. Rev. **163**, 816 (1967).
[11] S. M. Goodnick, D. K. Ferry, C. W. Wilmsen, Z. Liliental, D. Fathy, and O. L. Krivanek, Phys. Rev. B **32**, 8171 (1985).
[12] D. K. Ferry and S. M. Goodnick, in *Transport in Nanostructures* (Cambridge University Press, New York, 1997).
[13] T. Ando, A. B. Fowler, and F. Stern, Rev. Mod. Phys. **54**, 437 (1982).
[14] M. V. Fischetti and S. E. Laux, Phys. Rev. B **48**, 2244 (1993).
[15] F. Gámiz, J. A. López-Villanueva, J. A. Jiménez-Tejada, I. Melchor, and A. Palma, J. Appl. Phys. **75**, 924 (1994).
[16] F. Gámiz, J. A. López-Villanueva, J. Banqueri, J. E. Carceller, and P. Cartujo, IEEE Trans. Electron Devices **ED-42**, 258 (1994).
[17] J. B. Roldán, F. Gámiz, J. A. López-Villanueva, J. E. Carceller, and P. Cartujo, Semicond. Sci. Technol. **12**, 321 (1997).
[18] C. Jacoboni and L. Reggiani, Rev. Mod. Phys. **55**, 645 (1983).
[19] P. J. Price, Ann. Phys. (N.Y.) **133**, 217 (1981).
[20] H. Ezawa, Ann. Phys. (N.Y.) **67**, 438 (1971).
[21] M. V. Fischetti, F. Gámiz, and W. Hänsch, J. Appl. Phys. **92**, 7320 (2002).
[22] F. Gámiz, J. A. López-Villanueva, J. Banqueri, Y. Ghailan, and J. E. Carceller, Semicond. Sci. Technol. **10**, 592 (1994).